Transient Analysis of Coupled Natural Convection and Surface Thermal Radiation in a Tilted Open Cavity

J. F. Hinojosa* and M. E. Trujillo-Camacho

Department of Chemical Engineering and Metallurgy, University of Sonora, Blvd. Rosales y Luis Encinas, Hermosillo, Sonora, CP 83000, México

Abstract: Numeric results of the transient heat transfer by natural convection and surface thermal radiation in a tilted open cavity are presented. The conservation equations in primitive variables are solved using the finite volume method and the SIMPLEC algorithm. The transient results are obtained for a Rayleigh number of 10^6 and five inclination angles (0°, 45°, 90°, 120° and 180°. The numerical model predicts flow instabilities for inclination angle of 0°, which avoids reaching the steady state. The steady state is reached after a long time for ϕ=180°.

Keywords: Open cavity, transient natural convection, thermal radiation.

1. INTRODUCTION

In some solar concentration systems, the thermal receiver (open cavity) may have different orientations to allow the income of concentrated solar light. The above because a tracking system rotates the solar concentrator to maintain its optical axis pointing directly toward the sun. However, the dynamic of the fluid motion and the heat transfer depend of the inclination angle of the open cavity.

The investigations of the heat transfer by combined natural convection and surface thermal radiation in open cavities, are briefly presented next.

Lage *et al*. [1] studied numerically the heat transfer by natural convection and surface thermal radiation in a two-dimensional open top cavity. The authors solved separately the steady state equations of natural convection and thermal radiation, assuming a temperature distribution on the vertical adiabatic wall. Balaji and Venkateshan [2] obtained steady state numerical results for the interaction of surface thermal radiation with free convection in an open top cavity. They found that surface radiation alters substantially the basic flow pattern as well as the overall thermal performance substantially. Balaji and Venkateshan [3] developed a numerical study of combined conduction, natural convection and surface thermal radiation in an open top cavity. They found that surface radiation enhances overall heat transfer substantially (50–80%) depending on the radiative parameters. Singh and Venkateshan [4] presented a numerical study of steady combined laminar natural convection and surface two-dimensional side-vented open cavity. The numerical research provides evidence of the existence of thermal boundary layers along adiabatic walls of the cavity as a consequence of the interaction of natural convection and surface radiation.

Hinojosa *et al*. [5] presented numeric results for transient and steady-state natural convection and surface thermal radiation in a horizontal open square cavity. The results show that the radiative exchange between the walls and the aperture increases considerably the total average Nusselt number, from around 94% to 125%. Nouanegue *et al*. [6] studied conjugate heat transfer by natural convection, conduction and radiation in open cavities. The influence of the surface radiation provides a decreasing into the heat fluxes by natural convection and conduction while the heat flux by radiation increases when surface emissivity grows up. Hinojosa [7] reported the numerical calculations of heat transfer by natural convection and surface radiation in a tilted open shallow cavity. It was found that the exchange of thermal radiation between walls is considerably more relevant that the convective phenomenon for an inclination angle of 135°.

Wang *et al*. [8] studied the combined heat transfer by natural convection, conduction, and surface radiation in a side open cavity. The unsteady-state flow and heat transfer exhibited either periodic oscillating or chaotic behaviors due to formation of the thermal plumes at the bottom wall. Montiel-Gonzalez *et al.* [9] analyzed the validity of the Boussinesq approach for the heat transfer calculations in a side open cavity considering natural convection and surface thermal radiation. Numerical calculations were conducted for Rayleigh number (Ra) values in the range of 10^4-10^6. The temperature difference between the hot wall and

*Address correspondence to this author at the Department of Chemical Engineering and Metallurgy, University of Sonora, Blvd. Rosales y Luis Encinas, Hermosillo, Sonora, CP 83000, México; Tel: +52 (662) 2-29-21-06; Fax: +52 (662) 2-59-21-05; E-mail: fhinojosa@iq.uson.mx

E-ISSN: 2409-5826/15

the bulk fluid (ΔT) was varied among 10 and 100K. For total Nusselt numbers, the results with Boussinesq approach and variable properties, indicates deviations within 0.22% ($Ra=10^5$ and $\Delta T=10K$) and 5% ($Ra=10^4$ and $\Delta T=100K$).

Montiel-Gonzalez *et al.* [10] realized a theoretical and experimental study of steady-state heat transfer by natural convection and thermal radiation on a solar open cubic cavity-type receiver with a fixed orientation. Experimental results include air temperature measurements inside the receiver. These results are compared with theoretically obtained air temperatures, and the average deviation between both results is around 3.0%, when using the model with variable thermophysical properties, and is around 5.4% when using the Boussinesq approximation.

- The literature review indicates the absence of a detailed analysis for the transient heat transfer in tilted open cavities.
- This paper present the effect of inclination angle over the transient natural convection coupled with thermal radiation in a square open cavity.
- Detailed transient numerical calculations of the temperature fields and flow patterns are obtained and discussed.
- The manuscript provides valuable information to understand the dynamic behavior of heat transfer in tilted open cavities, which is relevant for thermal receivers of solar concentration systems.

2. PHYSICAL AND MATHEMATICAL MODELS

The heat transfer and the fluid flow in a two dimensional square tilted open cavity of length L, is considered in the present investigation (Figure **1**). The opposite wall to the aperture was kept to constant temperature (T_H=310 K), while the surrounding fluid interacting with the aperture was maintained to an ambient temperature (T_∞=300 K). The two remaining walls were considered adiabatic. The thermal fluid was air (Pr=0.71) and the flow was considered laminar. The fluid was assumed to be Newtonian, radiatively non-participating and the properties assumed constant except for the density in the buoyant force term in the momentum equations, according to the Boussinesq approximation. The walls of the cavity and the aperture were considered black bodies and diffuse emitters.

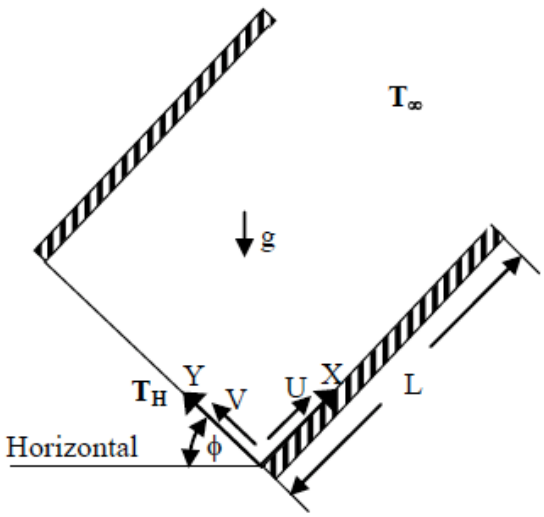

Figure 1: Scheme of the open tilted cavity.

The dimensionless conservation equations governing the transport of mass, momentum and energy in primitive variables are expressed as:

$$\frac{\partial U}{\partial X}+\frac{\partial V}{\partial Y}=0 \tag{1}$$

$$\frac{\partial U}{\partial \tau}+\frac{\partial (U^2)}{\partial X}+\frac{\partial (UV)}{\partial Y}=-\frac{\partial P}{\partial X}+\left(\frac{\Pr}{Ra}\right)^{1/2}\left(\frac{\partial^2 U}{\partial X^2}+\frac{\partial^2 U}{\partial Y^2}\right)+\theta\cos\phi \tag{2}$$

$$\frac{\partial V}{\partial \tau}+\frac{\partial (UV)}{\partial X}+\frac{\partial (V^2)}{\partial Y}=-\frac{\partial P}{\partial Y}+\left(\frac{\Pr}{Ra}\right)^{1/2}\left(\frac{\partial^2 V}{\partial X^2}+\frac{\partial^2 V}{\partial Y^2}\right)+\theta\sin\phi \tag{3}$$

$$\frac{\partial \theta}{\partial \tau}+\frac{\partial (U\theta)}{\partial X}+\frac{\partial (V\theta)}{\partial Y}=\frac{1}{(\Pr Ra)^{1/2}}\left(\frac{\partial^2 \theta}{\partial X^2}+\frac{\partial^2 \theta}{\partial Y^2}\right) \tag{4}$$

where $Ra=[g\beta(T_H-T_\infty)L^3]/\alpha\nu$ is the Rayleigh number, and $Pr = \nu/\alpha$ is the Prandtl number. The above equations were non-dimensionalized by defining

$$X=x/L,\ Y=y/L,\ \tau=U_o t/L,\ P=(p-p_\infty)/\rho U_o^2,\ U=u/U_o,\ V=v/U_o,\ \theta=(T-T_\infty)/(T_H-T_\infty) \tag{5}$$

The reference velocity U_o is related to the buoyancy force term and was defined as $Uo=(g\beta L(T_H-T_\infty))^{1/2}$.

The initial and the boundary conditions for the momentum and energy equations were considered as:

$P(X,Y,0)=U(X,Y,0)=V(X,Y,0)=\theta(X,Y,0)=0$

$U(0,Y,\tau)=V(0,Y,\tau)=U(X,0,\tau)=V(X,0,\tau)=U(X,1,\tau)=V(X,1,\tau)=0$

$$\left(\frac{\partial U}{\partial X}\right)_{X=1}=\left(\frac{\partial V}{\partial X}\right)_{X=1}=0$$

$\theta(0,Y,\tau)=1$

$\theta(1,Y,\tau)=0$ if U<0 or $\left(\frac{\partial\theta}{\partial X}\right)_{X=1}=0$ if U>0

$$\left(\frac{\partial\theta}{\partial Y}\right)_{Y=0,1}=N_rQ_r$$

In the mathematical formulation, $N_r=\sigma T_H^4L/k\left(T_H-T_\infty\right)$ is the dimensionless parameter of conduction radiation and $Q_r=q_r/\sigma T_H^4$ is the dimensionless net radiative heat flux on the corresponding adiabatic wall.

To obtain the net radiative heat fluxes over the walls, the radiosity-irradiance formulation was used, dividing the surface in elements according to the mesh used to solve the natural convection equations. View factors were evaluated using Hottel's crossed string method [11].

The average convective Nusselt number was computed integrating the temperature gradient over the heated wall as:

$$\overline{Nu}_c=\int_0^1-\frac{\partial\theta}{\partial X}dY \tag{6}$$

The average radiative Nusselt number was obtained integrating the dimensionless net radiative fluxes over the heated wall **[**12]:

$$\overline{Nu}_r=N_r\int_0^1Q_rdY \tag{7}$$

The total average Nusselt number was calculated by summing the average convective Nusselt number and the average radiative Nusselt number:

$$\overline{Nu}_t=\overline{Nu}_c+\overline{Nu}_r=\int_0^1-\frac{\partial\theta}{\partial X}dY+N_r\int_0^1Q_rdY \tag{8}$$

3. NUMERICAL METHOD OF SOLUTION

In order to obtain the results, a Fortran 90 code was developed. The equations (1-4) were discretized by integrating over staggered uniform control volumes. The convective terms were interpolated by the SMART scheme [13] and the diffusive terms with the central differencing scheme. The time discretization was made with the fully implicit scheme. Numerical solutions of the governing equations were obtained with the SIMPLEC algorithm [14]. The sets of linear algebraic equations were solved iteratively by the SIP method [15]. The iterative convergence for the variables was obtained in every time step.

However, because the coupling between the natural convection and the surface thermal radiation, the radiative balance was solved in every time step using an iterative method of subsequent approaches, from the information of the previous time step. The radiosities and net radiative fluxes were updated in every time step to obtain the corresponding thermal boundary conditions on the adiabatic walls.

Grid independent solutions were obtained by comparing the results of different grid meshes for Ra=1x10^6 and ϕ=90° in the steady state. The Figures **2a** y **2b** show the results for local values of the convective Nusselt number on the heated wall and U-velocity at the aperture. The difference between the calculations of 70x70 and 80x80 grid sizes was not significant, therefore the results were obtained with the 70x70 grid mesh. The dimensionless time step used for the calculations was 1x10^{-3}.

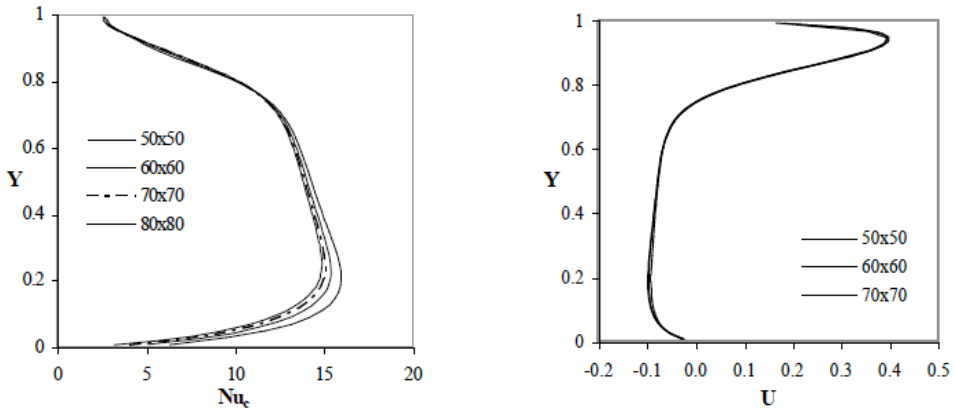

Figure 2: Grid independence study: (**a**) Local convective Nusselt numbers along the heated wall, (**b**) U-velocity at the aperture for different grid sizes.

The verification of the present code was accomplished by comparing the predictions with previous results reported in the literature. Table **1** show a comparison between the Nusselt numbers obtained with the present code and those reported by Montiel-Gonzalez *et al*. [10]. It can be observed that the absolute percentage difference with numerical results of average convective Nusselt number were between 0.6% ($Ra=10^5$) and 2.3% ($Ra=10^4$), whereas for average radiative Nusselt number were within 9.3% ($Ra=10^6$) and 13.4% ($Ra=10^4$). Based on above results the present numerical code was considered as verified.

Table 1: Comparison of Average Nusselt Numbers Reported in the Literature

	This work			Montiel-Gonzalez *et al.* [10] (ΔT=10K)		
Ra	$\overline{Nu}_c$	$\overline{Nu}_r$	$\overline{Nu}_t$	$\overline{Nu}_c$	$\overline{Nu}_r$	$\overline{Nu}_t$
10^4	3.72	6.70	6.70	3.05	3.34	2.98
10^5	8.02	14.42	14.42	6.36	7.34	6.40
10^6	17.29	29.72	29.72	12.32	15.82	12.43

4. RESULTS

The effect of inclination angle of the open cavity on the evolution in time of temperature fields and flow patterns is presented and discussed. The results were obtained for a Rayleigh number of 10^6 and five inclination angles (0°, 45°, 90°, 120° and 180°).

The transient results for the open cavity with an inclination angle of 0° are presented in Figure **2**. For τ=1, the isotherms indicate a heat transfer by conduction in a thin layer of fluid adjacent to the isothermal wall (the adiabatic walls are rapidly heated by the radiative exchange), as the heat transfer process continues the isotherms become curved near the bottom corners and the presence of symmetric thermal plumes is observed for τ=5. It is observed in τ=6-11, the symmetric ascending motion of thermal plumes next to the adiabatic vertical walls and the symmetric formation of new thermal plumes from the isothermal wall. The streamlines, for τ=1 to 5, show cold air incoming by the center of the aperture and the formation of vortexes closer to the adiabatic hot wall that move towards the aperture of the cavity. In interval time τ=12-18, the isotherms show thermal plumes growing up and moving to the aperture, until they leave the cavity. The streamlines from τ=12 to τ=18, show two vortexes in the bottom, their size increase with

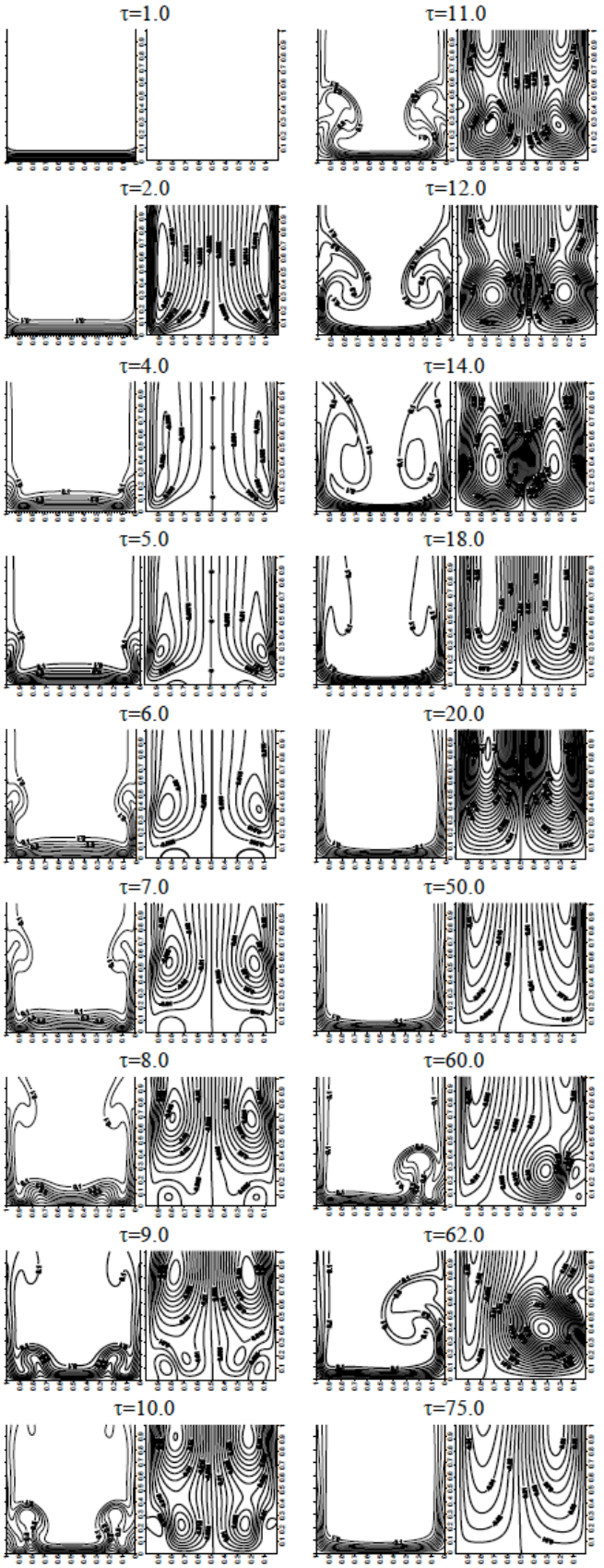

Figure 2: Time-evolution of the isotherms (left) and streamlines (right) in the open cavity with an inclination angle of 0° and a Rayleigh number of 10^6.

respect to, until they disappear and two symmetric zones of fluid motion are formed, the cold fluid enters by the center of the aperture and leaves adjacently to the adiabatic walls. However, from τ=20 to τ=50 apparently the steady state has been reached, but in τ=60 it is observed in the isotherms graph the formation of one thermal fluid in the right side of the isothermal wall and the next time (between t=60 and t=62) shows the increasing of its size and its movement toward the aperture to leave the cavity. The corresponding streamlines show the development of one vortex that grows up to cover almost half of right side of the cavity. The vortex is not present in τ=75.

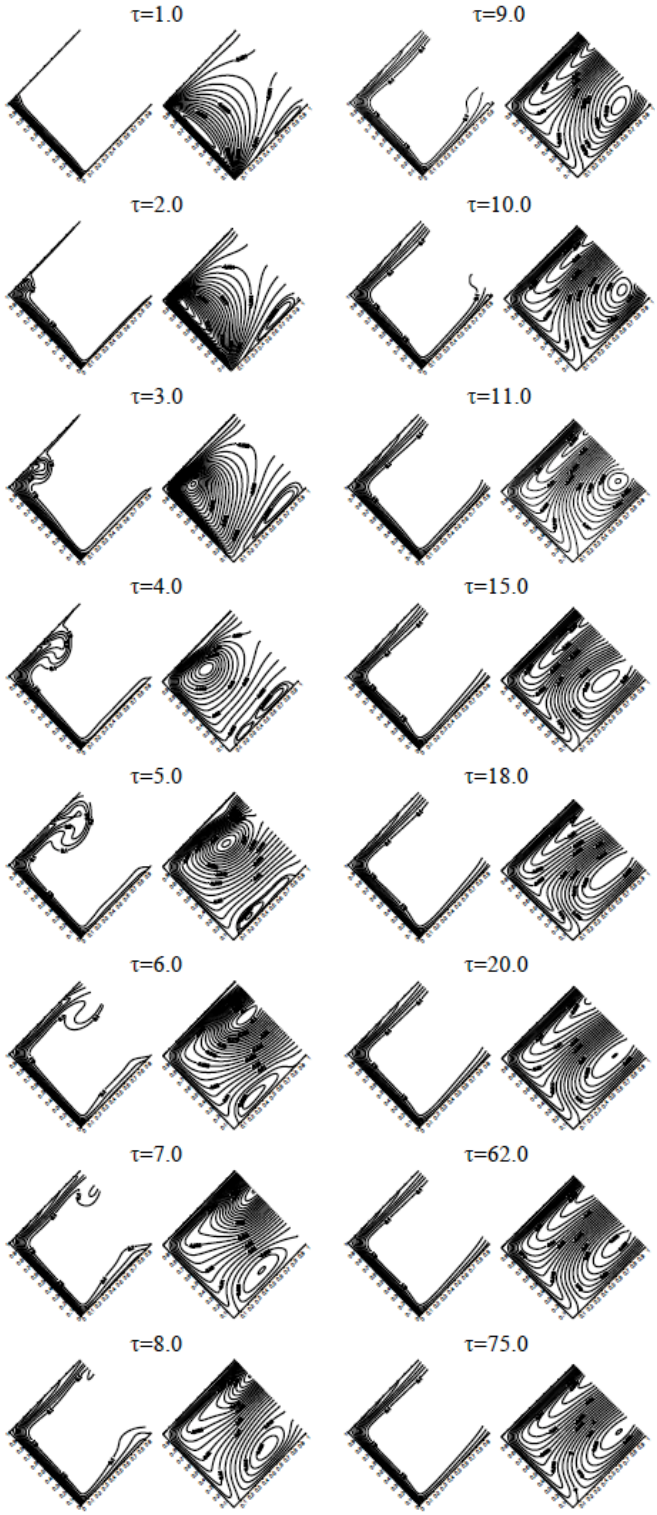

Figure 3: Time-evolution of the isotherms (left) and streamlines (right) in the open cavity with an inclination angle of 45° and a Rayleigh number of 10^6.

Figure **3** shows the transient results of isotherms and streamlines for a cavity with an inclination angle of 45°. For τ=1, the isotherms are parallel to the hot wall, with a small curvature near the top corner, at this time the streamlines show an elongated vortex adjacent to the isothermal wall. For τ=2 to 5, the isotherms indicate the motion of hot air from the top corner to the aperture, touching the top adiabatic wall. Whereas the streamlines show the displacement of the vortex (with a change in its shape and size), along the isothermal wall and the top adiabatic wall and the formation of a second vortex adjacent to the bottom adiabatic wall. However from τ=6 to τ=10, the heating of bottom adiabatic wall by the radiative exchange, increases the temperature of the incoming cold air, which is impelled to rise up. The above increases the size of the vortex on the bottom adiabatic wall. For τ=11 to 30, the temperature and fluid flow have minimum changes, therefore the steady state has been reached. The isotherms show a thin boundary layer over the bottom adiabatic wall formed by the incoming cold air and another boundary layer adjacent to the isothermal wall formed by the hot air impelled by the buoyancy force. On the other hand the streamlines show two different circulations of the incoming air: (a) the cold air enters but before reaching the isothermal wall, turns to the aperture and goes out near to the bottom adiabatic wall, (b) the incoming air reaches the hot wall near to the bottom wall and ascends by the isothermal wall and moves to the aperture adjacent to the top adiabatic wall.

Figure **4** shows transient results from τ=1 to 50, for a cavity with an inclination angle of 90°. For τ=1, the isotherms were parallel to the hot wall but as the heat transfer process continues the thermal field becomes curved. Also, the formation of thermal boundary layers is observed in all walls. Looking at the streamlines, for τ=1 to 5, one vortex appears very close to the hot wall and moves toward the top adiabatic wall, afterwards it moves towards the aperture of the cavity leaving it at τ=6. For τ=8 at the bottom wall begins a small thermal plume that grows up and moves toward the vertical hot wall. When it reaches the hot wall, the thermal plume

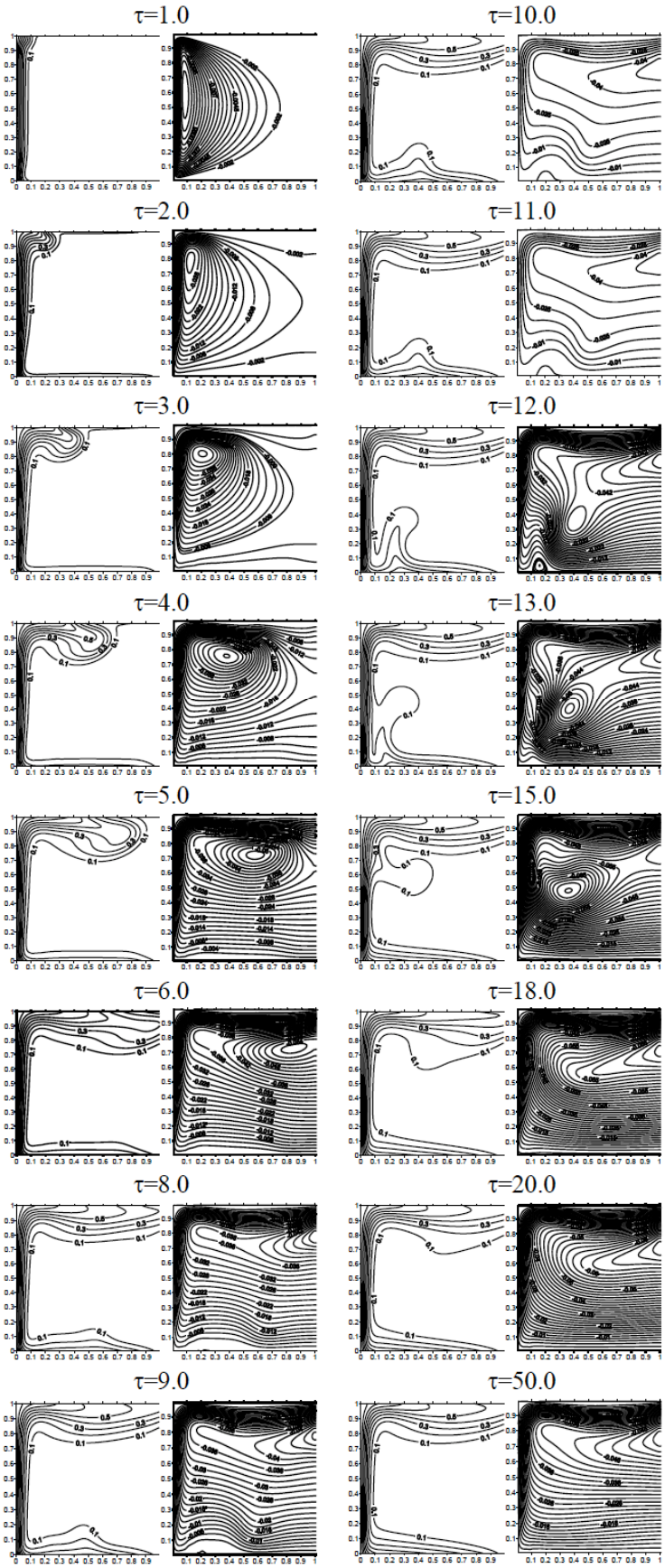

Figure 4: Time-evolution of the isotherms (left) and streamlines (right) in the open cavity with an inclination angle of 90° and a Rayleigh number of 10^6.

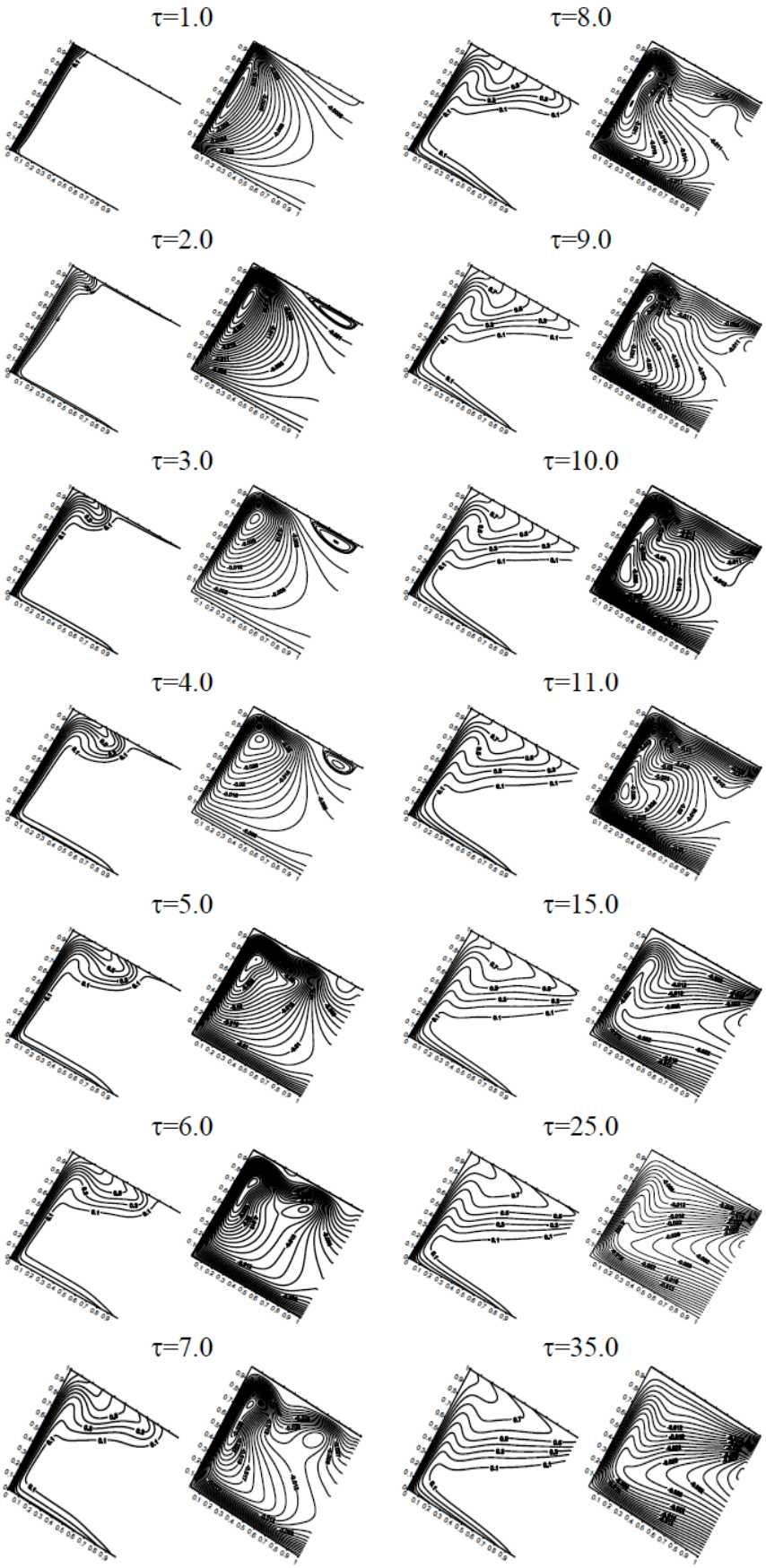

Figure 5: Time-evolution of the isotherms (left) and streamlines (right) in the open cavity with an inclination angle of 120° and a Rayleigh number of 10^6.

mixes with the thermal boundary layer of the hot wall and moves toward the top wall. Then, the thermal plume again mixes with the thermal boundary layer of the top adiabatic wall and moves toward the aperture. For τ=10, a secondary vortex appears at the vicinity of the left bottom corner of the open cavity. This new small vortex eventually disappears at τ=13. However, another vortex appears at the center of the cavity at τ=11, and it grows up and moves toward to the opening and leaves the cavity at τ=18.

The time sequence of both isotherms and streamlines in the open cavity with an inclination angle of 120° is presented in Figure **5**. Again the heat transfer seems to start with the heat conduction mechanism as it can be seen in τ=1, since the

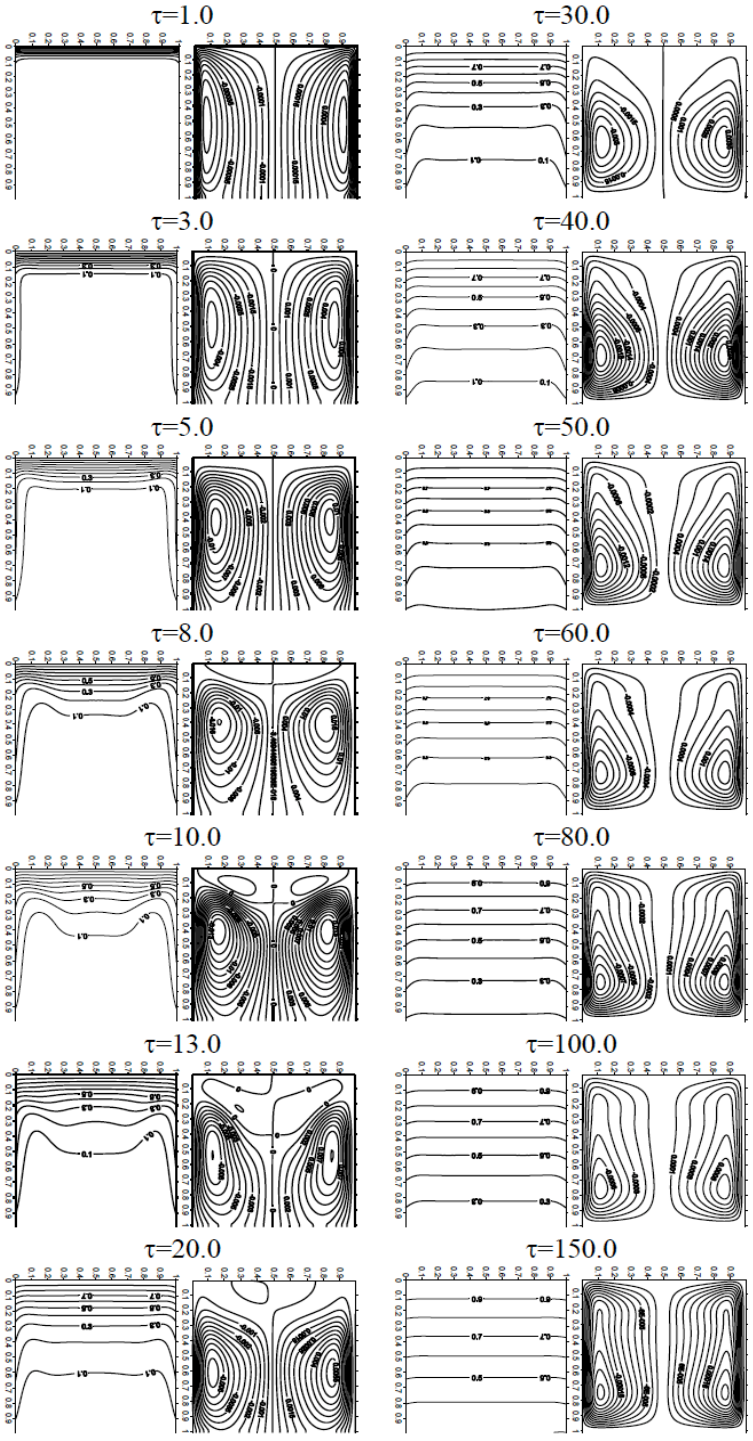

Figure 6: Time-evolution of the isotherms (left) and streamlines (right) in the open cavity with an inclination angle of 180° and a Rayleigh number of 10^6.

isotherms are parallel to the hot wall (with a small curvature at the top corner), however the streamlines show that at this time both an elongated vortex adjacent to the isothermal wall and a small vortex on the top adiabatic wall have been formed. The time sequence between τ=2 and τ=9 of the isotherms, shows that the heating of fluid adjacent to the adiabatic walls caused by the incidence of thermal radiation, and the motion of hot air from the top corner to the aperture in an oblique way. The corresponding streamlines show a change in the size and shape of the vortex located in front of the isothermal wall. For τ=10 to τ=20 the isotherms graphs show small variations, they indicate a heating of the incoming air by the bottom adiabatic wall, the presence of a thermal boundary layer next to the isothermal wall and an oblique thermal stratification formed by the outgoing air. On the other hand, the streamlines exhibit that the vortexes disappear after τ=15 and the flow patterns remains practically constant.

The transient results for an inclination angle of 180° are presented in Figure **6**. For τ=1, the isotherms are parallel and very close to the isothermal wall, and for τ=3-5 the effect of the thermal radiation on adiabatic wall heating is observed and also is visible a separation of isotherms from the isothermal wall. The streamlines show the formation of two big counter rotating vortexes. When time increases (t=8-30), the separation of isotherms shows that the heat diffusion is happening, until that at τ=150 the isotherms are almost equally spaced indicating a heat transfer dominated by heat conduction.

Figure **7** shows the variation of average total Nusselt number with respect to time for the five inclination angles of the open cavity (0°, 45°, 90°, 120° and 180°). It can be observed that for most inclination angles (45°, 90°, 120° and 180°), the initial Nusselt numbers are very high, but they reduce with respect to time and tend to a constant value. For ϕ=45°, 90° and 120°, the steady state is reached after τ=35, however for ϕ=180° is reached after τ=180. On the other hand the average total Nusselt number for the open cavity (ϕ=0°) has an erratic behavior, therefore the steady state is not reached.

5. CONCLUSIONS

In this paper, transient numerical results of the heat transfer by natural convection and surface thermal radiation in a tilted open cavity are presented and analyzed. From the results, the following conclusions were obtained:

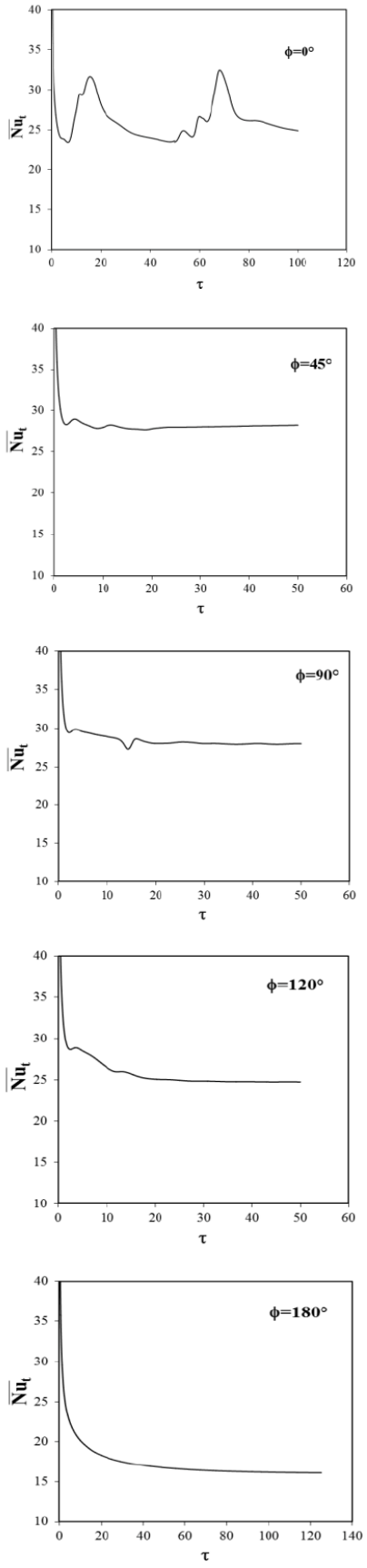

Figure 7: History of the average total Nusselt number for different inclination angles of the open cavity (0°, 45°, 90°, 120° and 180°) and a Rayleigh number of 10^6.

1. The formation of multiple thermal plumes in the isothermal wall for an inclination angle of 0^{o} causes oscillations in the total Nusselt number and avoids to reach the steady state.

2. The steady state for ϕ=180° is reached after longer time (τ=180); whereas for ϕ=45°, 90° and 120°, which is reached after τ=35.

3. The history of the temperature field and the flow pattern is very sensitive about the orientation of the cavity.

REFERENCES

[1] Lage JL, Lim JS and Bejan A. Natural convection with radiation in a cavity with open top end. J Heat Trans-T ASME 1992; 114: 479-486. http://dx.doi.org/10.1115/1.2911298

[2] Balaji C and Venkateshan SP. Interaction of radiation with free convection in an open cavity. Int J Heat Fluid Flow 1994; 15: 317-324. http://dx.doi.org/10.1016/0142-727X(94)90017-5

[3] Balaji C and Venkateshan SP. Combined conduction, convection and radiation in a Slot. Int J Heat Fluid Flow 1995; 16: 139. http://dx.doi.org/10.1016/0142-727X(94)00014-4

[4] Singh SN and Venkateshan SP. Numerical study of natural convection with surface radiation in side-vented open cavities. Int J Therm Sci 2004; 43: 865-876. http://dx.doi.org/10.1016/j.ijthermalsci.2004.01.002

[5] Hinojosa JF, Cabanillas RE, Alvarez G and Estrada CA. Numerical study of transient and steady-state natural convection and surface thermal radiation in a horizontal square open cavity. Numer Heat Tr A-Appl 2005; 48: 179-196. http://dx.doi.org/10.1080/10407780590948936

[6] Nouaneguea H, Muftuoglua A and Bilgen E. Conjugate heat transfer by natural convection, conduction and radiation in open cavities. Int J Heat Mass Transfer 2008; 51: 6054-6062. http://dx.doi.org/10.1016/j.ijheatmasstransfer.2008.05.009

[7] Hinojosa JF. Natural convection and surface thermal radiation in a tilted open shallow cavity. Revista Mexicana de Física 2012; 58: 19-28.

[8] Wang Z, Yang M and Zhang Y. Oscillation and chaos in combined heat transfer by natural convection, conduction, and surface radiation in an open cavity. Journal of Heat Transfer 2012; 134: 09450. http://dx.doi.org/10.1115/1.4006269

[9] Montiel-González M, Hinojosa-Palafox J and Estrada-Gasca CA. Numerical study of the Boussinesq approach validity for natural convection and surface thermal radiation in an open cavity. Revista Mexicana de Física 2013; 59: 594-605.

[10] Montiel-González M, Hinojosa JF, Villafán-Vidales HI, Bautista-Orozco A and Estrada CA. Theoretical and experimental study of natural convection with surface thermal radiation in a side open cavity. Applied Thermal Engineering 2015; 75: 1176-1186. http://dx.doi.org/10.1016/j.applthermaleng.2014.05.047

[11] Modest M. Radiative Heat Transfer, 2nd ed., McGraw-Hill, New York, USA 1993.

[12] Akiyama M and Chong QP. Numerical analysis on natural convection with surface radiation in a square enclosure. Numerical Heat Transfer Part A 1997; 33: 419-433. http://dx.doi.org/10.1080/10407789708913899

[13] Gaskell PH and Lau AKC. Curvature-compensated convective transport: SMART, a new boundedness-preserving transport algorithm. International Journal of Numerical Methods in Fluids 1988; 8: 617-641. http://dx.doi.org/10.1002/fld.1650080602

[14] Van Doormaal JP and Raithby GD. Enhancements of the SIMPLE method for predicting incompressible fluid flows. Numerical Heat Transfer 1984; 7: 147-163. http://dx.doi.org/10.1080/01495728408961817

[15] Stone H. Iterative solution of implicit approximation of multi-dimensional partial differential equations. Journal of Numerical Analysis 1968; 5: 530-558. http://dx.doi.org/10.1137/0705044

Received on 26-10-2015 Accepted on 13-12-2015 Published on 31-12-2015

DOI: http://dx.doi.org/10.15377/2409-5826.2015.02.02.1